

Title	Surface segregation during injection molding of polycarbonate/poly(methyl methacrylate) blend
Author(s)	Sako, Takumi; Ito, Asae; Yamaguchi, Masayuki
Citation	Journal of Polymer Research, 24(6): Article:89
Issue Date	2017-05-09
Type	Journal Article
Text version	author
URL	<a href="http://hdl.handle.net/10119/15298">http://hdl.handle.net/10119/15298</a>
Rights	This is the author-created version of Springer, Takumi Sako, Asae Ito, Masayuki Yamaguchi, Journal of Polymer Research, 24(6), 2017, Article:89. The original publication is available at <a href="http://www.springerlink.com">www.springerlink.com</a> , <a href="http://dx.doi.org/10.1007/s10965-017-1251-2">http://dx.doi.org/10.1007/s10965-017-1251-2</a>
Description	

# Surface segregation during injection molding of polycarbonate/poly(methyl methacrylate) blend

Takumi Sako, Asae Ito, and Masayuki Yamaguchi\*

School of Materials Science,  
Japan Advanced Institute of Science and Technology,  
1-1 Asahidai, Nomi, Ishikawa 923-1292, JAPAN

## Acknowledgments

A part of this work was supported by JSPS Grant-in-Aid for Scientific Research (B) Grant Number 16H04201.

## Abstract

We investigated the distribution of the constituent polymers of an injection-molded product comprising a miscible blend of polycarbonate (PC) and low-molecular-weight poly(methyl methacrylate) (PMMA). We found that PMMA became localized at the surface without affecting the transparency of the product. As a result, the surface hardness was effectively enhanced by a small amount of PMMA. This technique can be used to produce an ideal plastic glass that has high transparency, mechanical toughness, and high surface hardness.

**Keywords:** Segregation; Polymer blend; Injection molding; Polycarbonate; Poly(methyl methacrylate)

---

\*Correspondence to Masayuki Yamaguchi  
Phone: +81-761-51-1621; Fax: +81-761-51-1149  
E-mail: m\_yama@jaist.ac.jp

## Introduction

Polycarbonate (PC) shows good heat resistance and mechanical toughness, but its surface properties such as hardness and scratch resistance require improvement. In contrast, poly(methyl methacrylate) (PMMA) has marked surface hardness and scratch resistance, but has poor mechanical toughness and a low glass transition temperature  $T_g$ . Therefore, the surface localization of PMMA in a miscible PC/PMMA blend will create an ideal plastic glass with good transparency, scratch resistance, heat resistance, and mechanical toughness. In general, PMMA is known to be miscible with PC when the molecular weight is low [1-3]. Some blend films prepared by a solution-cast method also show a single  $T_g$ , although blends prepared by melt-mixing are immiscible when both materials have high molecular weight [4-12]. Furthermore, the acceleration of transesterification reaction [11] and the exposure to radiation beam [12] also enhance the miscibility. Moreover, multilayered films composed of PMMA and PC can be fabricated by co-extrusion [13] or lamination with an adhesive [14].

Various attempts have been carried out to localize one component at the surface of a polymer blend to provide desirable surface properties. One well-known example is a solution-cast film, in which the difference in the surface tension and/or the solubility with the solvent is responsible for surface segregation. This phenomenon has been reported in blends of polystyrene (PS) and PMMA [15, 16], and also in PC/PMMA blends [5]. Moreover, our research group reported that a low-molecular-weight fraction in polyethylene with a broad molecular weight

distribution is segregated in the high-temperature region during annealing under a temperature gradient [17]. Such segregation behavior has also been detected in miscible blends of PC and low-molecular-weight PMMA when the annealing temperature is lower than LCST. In this case, the PMMA content is high at the high temperature side and vice versa [3]. Although this method provides a superior product comprising PC/PMMA blends with a large amount of PMMA at one surface, it is not ideal for industrial applications because it involves a prolonged annealing process, e.g., one hour.

Segregation also occurs in miscible blends that are subjected to shear flow [18-25]. According to Onuki, shear-induced phase separation results from variations in viscosity due to composition fluctuations, which lead to relative motion between the two components [20]. Therefore, segregation tends to occur in blends with marked differences in shear viscosity between components, e.g., blends of a polymer and a plasticizer [18-25]. In contrast, shear-induced mixing also occurs [25-28]. Such phenomena were explained also by the concept of the excess energy stored in polymer chains under flow field [21,25-27]. Because most polymer goods are produced under shear flow, the phenomenon should be given serious consideration. Piscioti et al. found that the plasticizer content is high at the surface of plasticized PS [23]. Because the shear rate is the greatest at the wall of a mold, the surface segregation of a plasticizer reduces the total stress during processing and enhances flowability such as spiral flow length. Therefore, there is a great potential for employing shear-induced segregation to obtain products with specific surface properties.

In this study, we investigated the segregation behavior during injection-molding in a miscible polymer blend comprising PC and low-molecular-weight PMMA.

## Experimental

### Materials and sample preparation

We used a commercially available bisphenol A polycarbonate (the PC) (Panlite® L-1225Y; Teijin Ltd., Japan) and PMMA kindly prepared by Mitsubishi Rayon. The molecular weights of the polymers were  $M_n = 28,000$  and  $M_w = 46,000$  for PC, and  $M_n = 8,900$  and  $M_w = 15,000$  for PMMA (evaluated using size exclusion chromatography equipment (HLC-8020; Tosoh Corp., Japan) with polystyrene standard samples). The polymers were blended using a co-rotating twin-screw extruder (ULT nano 15TW; Technovel Corp., Japan). The melt temperature was 260°C and the rotational speed of the screw was 30 rpm. The blended sample was extruded from a circular die with a diameter of 2 mm. Subsequently, the extruded strand was cooled in a water bath and cut into pellets by a strand cutter.

The pellets were fed into an injection-molding machine (HM7; Nissei Plastic Industrial Co., Ltd., Japan) to produce a  $70 \times 10 \times 2.0 \text{ mm}^3$  rectangular specimen. The temperatures of the barrel and mold were 280 and 80°C, respectively.

Compression-molded films were also prepared using a compression-molding machine (SA303IS; Tester Sangyo Co., Ltd., Japan) for 3 min at 10 MPa. The heating and cooling temperatures were 280 and 80°C, respectively.

## Measurements

The dependence on temperature of the tensile storage and tensile loss moduli ( $E'$  and  $E''$ , respectively) were investigated using a dynamic mechanical analyzer (E-4000; UBM Co., Ltd., Japan) at 30–180°C. The frequency was 10 Hz and the heating rate was 2°C/min. A  $5 \times 10 \times 0.3 \text{ mm}^3$  rectangular specimen was cut from the compression-molded film.

The dependence on angular frequency of the shear storage and shear loss moduli ( $G'$  and  $G''$ , respectively) in the molten state were investigated using a cone-and-plate rheometer (AR2000; TA Instruments Corp., USA) at 280°C. The angle of the cone was 4° and the diameter was 25 mm.

The blend composition at the surface of the injection-molded products was investigated by attenuated total reflectance Fourier-transform infrared spectroscopy (ATR-FTIR) (Spectrum 100 Optica FT-IR spectrometer; PerkinElmer Inc., USA) using thallium bromoiodide (KRS-5) and germanium (Ge) as ATR crystals. The refractive indices of KRS-5 and Ge are 2.4 and 4.0, respectively. PC/PMMA samples of various compositions were also investigated to obtain a calibration curve for the evaluation of PMMA content.

Number- and weight-average molecular weights at the surface and core of the injection-molded products were evaluated by size exclusion chromatography (HLC-8020 instrument; Tosoh Corp.) at 40°C using chloroform as a solvent at a flow rate of 1.0 mL/min. The surface was ground to an approximate depth of 50  $\mu\text{m}$  using a metal file to collect samples of the surface material.

Surface hardness was measured using a type D durometer (Japanese Standards Association standard JIS K 6253) (CL-150 Constant Load Durometer; Kobunshi Keiki Co., Ltd., Japan) at room temperature.

## Results and Discussion

We evaluated the dependence on temperature of  $E'$  and  $E''$  of the compression-molded samples to determine miscibility. It is well known that PC/PMMA blends have a lower critical solution temperature (LCST) [7,15-17].

[Figure 1]

As shown in Figure 1, the glass transition temperature ( $T_g$ ), which was determined by the peak temperature in the  $E''$  curve in this study, was detected as follows; 162°C for pure PC, 97°C for pure PMMA [3], and 151°C for PC/PMMA (95/5). Apparently,  $T_g$  was lowered by the addition of PMMA. Moreover, no peak could be ascribed to  $T_g$  in the pure PMMA, demonstrating that the blend is miscible at the processing temperature, i.e., 280°C. The injection-molding procedures were carried out at the same temperature, so the products should both have been transparent. These results indicate that LCST is higher than 280°C at this blend ratio, which corresponds with our previous study [3]. Furthermore, the room-temperature  $E'$  was slightly enhanced by the addition of PMMA, which met the demand for PC [29, 30]. This result suggests that surface hardness is effectively enhanced by the surface localization of PMMA in a blend.

The dependence on frequency of  $G'$  and  $G''$  at 280°C, i.e., the processing

temperature, for the individual pure samples is illustrated in Figure 2. Because the phase difference is large with a low modulus, we could not evaluate the  $G'$  of PMMA. As shown in the figure, the  $G''$  of PMMA was significantly lower than that of PC. The zero-shear viscosities of PC and PMMA at 280°C were 1000 Pa·s and 1 Pa·s, respectively. Because they are miscible, PMMA acts as plasticizer at this temperature.

[Figure 2]

A photograph of the injection-molded products of pure PC and PC/PMMA is shown in Figure 3. Both samples had marked transparency. This result corresponds to the dynamic mechanical properties.

[Figure 3]

The PMMA content at the surface of the injection-molded product was evaluated by ATR-FTIR measurements. Figure 4 shows the FT-IR spectra of the blend and individual pure components. The peak intensity at  $1,436\text{ cm}^{-1}$ , ascribed to the bending vibration of the C-H bonds in the  $\text{CH}_3$  groups in PMMA, and that at  $1,770\text{ cm}^{-1}$ , ascribed to the stretching of the carbonyl groups in PC, were used for the characterization [3]. The peak intensity ratio was denoted as  $A_{\text{PMMA}}/A_{\text{PC}}$ . Prior to the investigation of the injection-molded product, the peak intensity ratios were evaluated using compression-molded plates of various blend compositions (100/0, 95/5, 90/10, 80/20, 50/50, and 0/100) to obtain the calibration curve shown in Figure 5.

[Figure 4] [Figure 5]

The peak intensity ratios at the surface of the PC/PMMA (95/5) injection-molded product are summarized in Table 1, and the PMMA contents estimated using the



calibration curve are also listed. The measurements were performed at two different points, as shown in Figure 3. Both KRS-5 and Ge were used as ATR crystals to obtain the information on the depth profile of the blend composition. The penetration depth ( $d_p$ ) of the IR beam was calculated using equation 1:

$$d_p = \frac{\lambda}{2\pi\sqrt{\sin^2 \theta - (n_2 - n_1)^2}} \quad (1)$$

where  $\lambda$  is the wavelength of the infrared beam,  $n_1$  and  $n_2$  are the refractive indices of the sample and the ATR crystal, respectively, and  $\theta$  is the incidence angle of the infrared beam. The  $d_p$  values under these experimental conditions were approximately 1  $\mu\text{m}$  for KRS-5 and 0.3  $\mu\text{m}$  for Ge.

[Table 1]

As shown in the figure, the PMMA content obtained using the Ge crystal was obviously higher than that obtained using KRS-5, and almost twice as high as the average (5%). This clearly indicates that the PMMA content at the surface of the injection-molded product was high. Considering that the content determined using the KRS-5 crystal was approximately 5%, i.e., the original composition, the segregation became significant in the thin surface region ( $\sim 1 \mu\text{m}$ ). Furthermore, there was no difference in PMMA content between P1 and P2, suggesting that the surface localization of PMMA occurs over the whole surface of the injection-molded product.

To confirm the segregation behavior, we evaluated molecular weights by size exclusion chromatography. As shown in Figure 6, the material from the surface region had a low molecular weight compared with that from the core region, which supports

the surface segregation of PMMA. Because grinding was performed to a depth of 50  $\mu\text{m}$  from the surface, the “surface” sample contained a large amount of “core” material, as suggested by the difference in ATR spectra between Ge and KRS. However, the difference in Figure 6 is obvious, although there is a possibility of degradation to some extent. If the measurements had been carried out using a sample collected at a smaller depth, the difference between the molecular weights would have been pronounced.

[Figure 6]

Such segregation behavior could occur by the shear-induced phase separation, although the blend sample is transparent. Shear-induced phase separation is considered to be originated from the positive deviation of stored energy of polymer chains from the sum of the stored energies of the respective components [21,25-27]. Considering that shear-induced phase separation was often reported for blends with a plasticizer [19-25], a large difference in the shear viscosity plays an important role of this phenomenon. Furthermore, the surface segregation of a low-viscous component, i.e., PMMA, leads to the enhancement of flowability such as spiral flow at injection-molding.

We expected hardness to be enhanced by the addition of PMMA and its segregation at the surface. Therefore, we measured type D durometer hardness. As shown in Figure 7, the PC/PMMA (95/5) compression-molded product was harder than the pure PC product. Furthermore, it should be noted that the PC/PMMA (95/5) injection-molded product was harder than the corresponding compression-molded

product, which can be attributed to the surface localization of PMMA.

[Figure 7]

## **Conclusion**

We examined the structure and properties at surface of the injection-molded product of a miscible blend comprising PC and low-molecular-weight PMMA. The ATR-FTIR measurements revealed that the surface region had a higher PMMA content, which was obvious when Ge was employed for the ATR crystal. The surface segregation of PMMA was also supported by the molecular weight measurements. The segregation behavior could be attributed to the shear-induced phase separation, which is attributed to the excess stored energy of polymer chains during flow. The high shear rate near the mold wall could be responsible for the structure change. Furthermore, this phenomenon indicates that the flowability is improved by the addition of the PMMA. The surface hardness was effectively enhanced by the surface localization of PMMA. Because PC is mainly processed by injection-molding, this technique will have important information to develop advanced PC materials in the industry.

## **Reference**

1. Butzback GD, Wendorff JH (1991) *Polymer* 32:1155
2. Nishimoto M, Keskkula H, Paul DR (1991) *Polymer* 32:272
3. Sako T, Nobukawa S, Yamaguchi M (2015) *Polym J* 47:576

4. Saldanha JM, Kyu T (1987) *Macromolecules* 20:2840
5. Lhoest JB, Bertrand P, Weng LT, Dewez JL (1995) *Macromolecules* 28:4631.
6. Woo EM, Su CC (1996) *Polymer* 37:4111
7. Agari Y, Ueda A, Omura Y, Nagai S (1997) *Polymer* 38:801
8. Ray SR, Bousmina M, Maazouz A (2006) *Polym Eng Sci* 46:1121
9. An N, Yang Y, Dong L (2007) *Macromolecules* 40:306
10. Singh AK, Mishra RK, Prakash R, Maiti P, Singh AK, Pandey D (2010) *Chem Phys Lett* 486:32
11. Singh AK, Prakash R, Pandey D (2011) *J Phys Chem* 115:1601
12. Magida MM (2012) *J Appl Polym Sci* 125:3184
13. Scholtyssek S, Seydewitz V, Adhikari R, Pfeifer F, Michler GH, Siesler HW (2013) *J Appl Polym Sci* 127:4262
14. Antoine GO, Batra RC (2014) *Comp Structures* 116:193
15. Kajiyama T, Tanaka K, Takahara A (1998) *Macromolecules* 31:3746
16. Ton-That C, Shard AG, Teare DOH, Bradley RH (2001) *Polymer* 42:1121
17. Siriprumpoonthum M, Mieda N, Nobukawa S, Yamaguchi M (2011) *J Polym Res* 18:2449
18. Helfand E, Fredrickson GH (1989) *Phys Rev Lett* 62:2468
19. Yanase H, Moldenaers P, Mewis J, Avetz V, van Egmond JW, Fuller GG (1991) *Rheol Acta* 30:89
20. Onuki A (1995) *Intern J Thermophys* 16:381
21. Sootaranun W, Higgins JS, Papathanasiou TD (1996) *Fluid Phase Equilibria*

121:273

22. Kume T, Hattori H, Hashimoto T (1997) *Macromolecules* 30:427
23. Pisciotti F, Lausmaa J, Boldizar A, Rigdahl A (2003) *Polym Eng Sci* 43:1289
24. Murase H, Kume T, Hashimoto T, Ohta Y (2005) *Macromolecules* 38:8719
25. Ougizawa T, Morphology of Polymer Blends, in *Polymer Blends Handbook*, 2<sup>nd</sup> Edition, Eds. Utracki LA, Wilkie CA (2014) Springer, pp.875-918
26. Wolf BA (1984) *Macromolecules* 28:1144
27. Kammer HW, Kummerloewe C, Kressler J, Melior JP (1991) *Polymer* 32:1488
28. Madbouly S, Ohmomo M, Ougizawa T, Inoue T (1999) *Polymer* 40:1465
29. Sako T, Miyagawa A, Yamaguchi M (2017) *J Appl Polym Sci* in press (DOI: 10.1002/app.44882)
30. Miyagawa A, Ayerdura V, Nobukawa S, Yamaguchi M (2016) *J Polym Sci Polym Phys Ed* 54:2388

Figure Caption

Figure 1 Temperature dependence of tensile storage modulus  $E'$  and loss modulus  $E''$  at 10 Hz for compression-molded products; (closed symbols) PC and (open symbols) PC/PMMA (95/5).

Figure 2 Frequency dependence of shear storage modulus  $G'$  and loss modulus  $G''$  at 280°C; (closed symbols) PC and (open symbols) PC/PMMA (95/5).

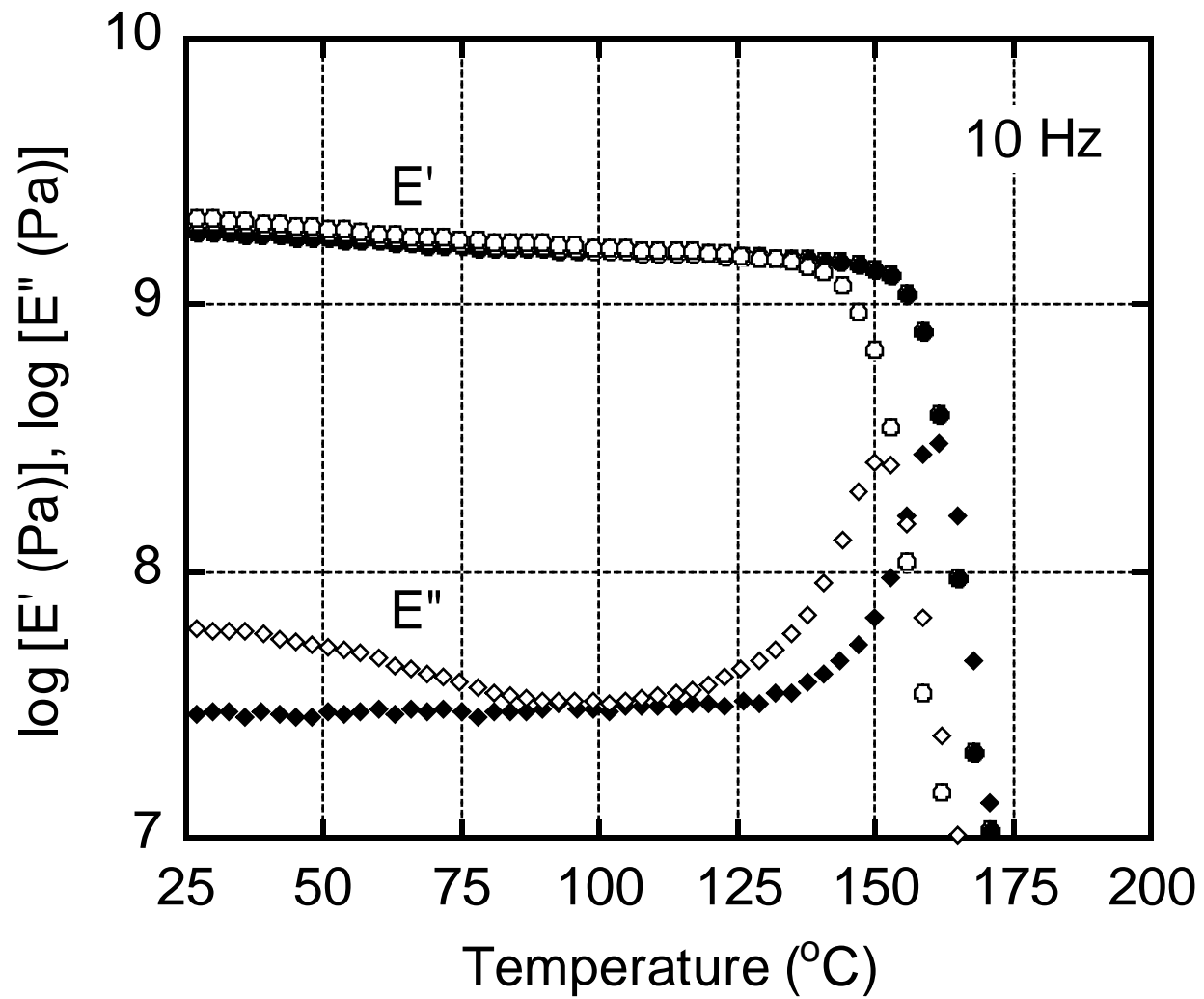
Figure 3 Photograph of injection-molded products of (left) PC and (right) PC/PMMA (95/5).

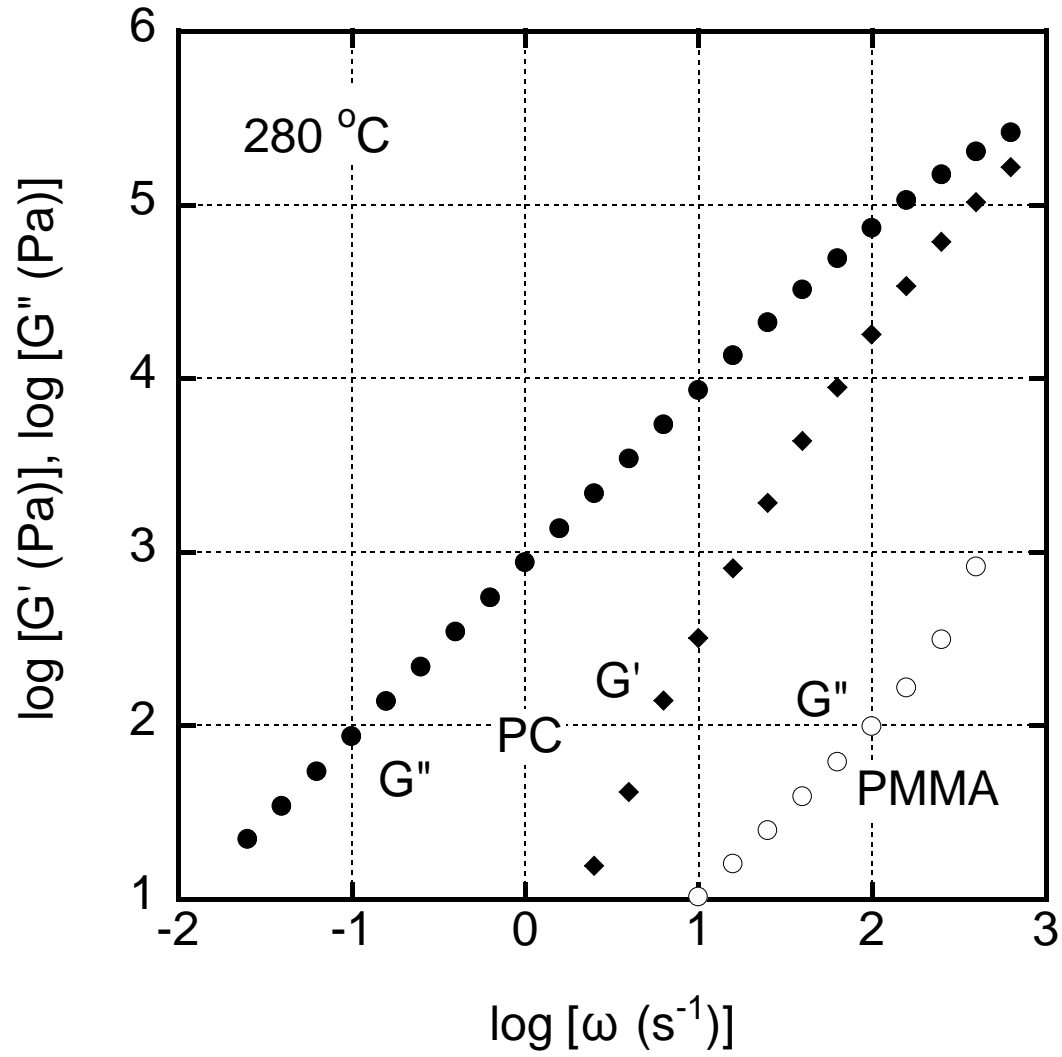
Figure 4 FT-IR spectra for compression-molded plates of pure PC, pure PMMA, and PC/PMMA (95/5).

Figure 5 Calibration curve to calculate the PMMA content in the blend.

Figure 6 SEC curves of the PC/PMMA (95/5) injection-molded product; (solid line) surface region and (dotted line) core region.

Figure 7 Durometer (D) hardness of the PC injection-molded product, the PC/PMMA (95/5) compression-molded product, and the PC/PMMA (95/5) injection-molded product.

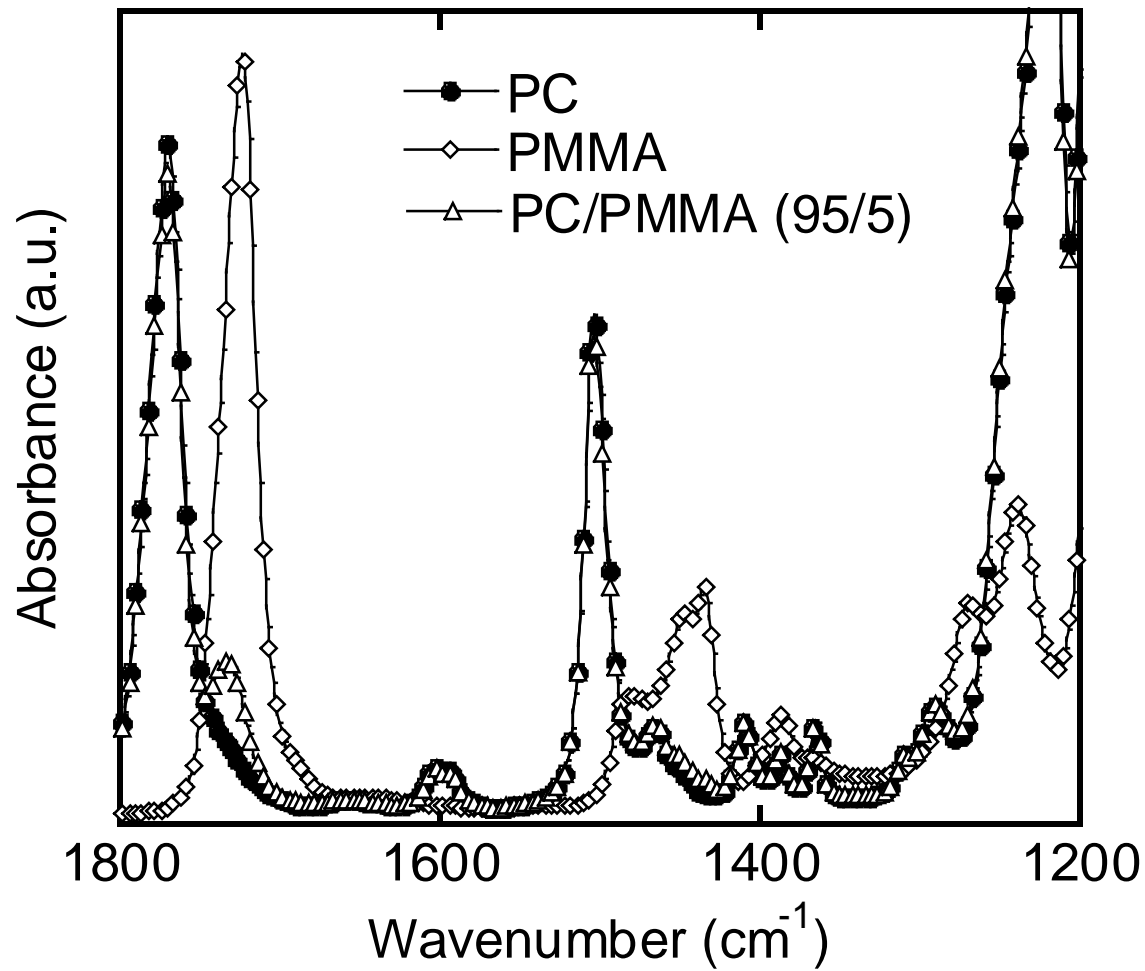


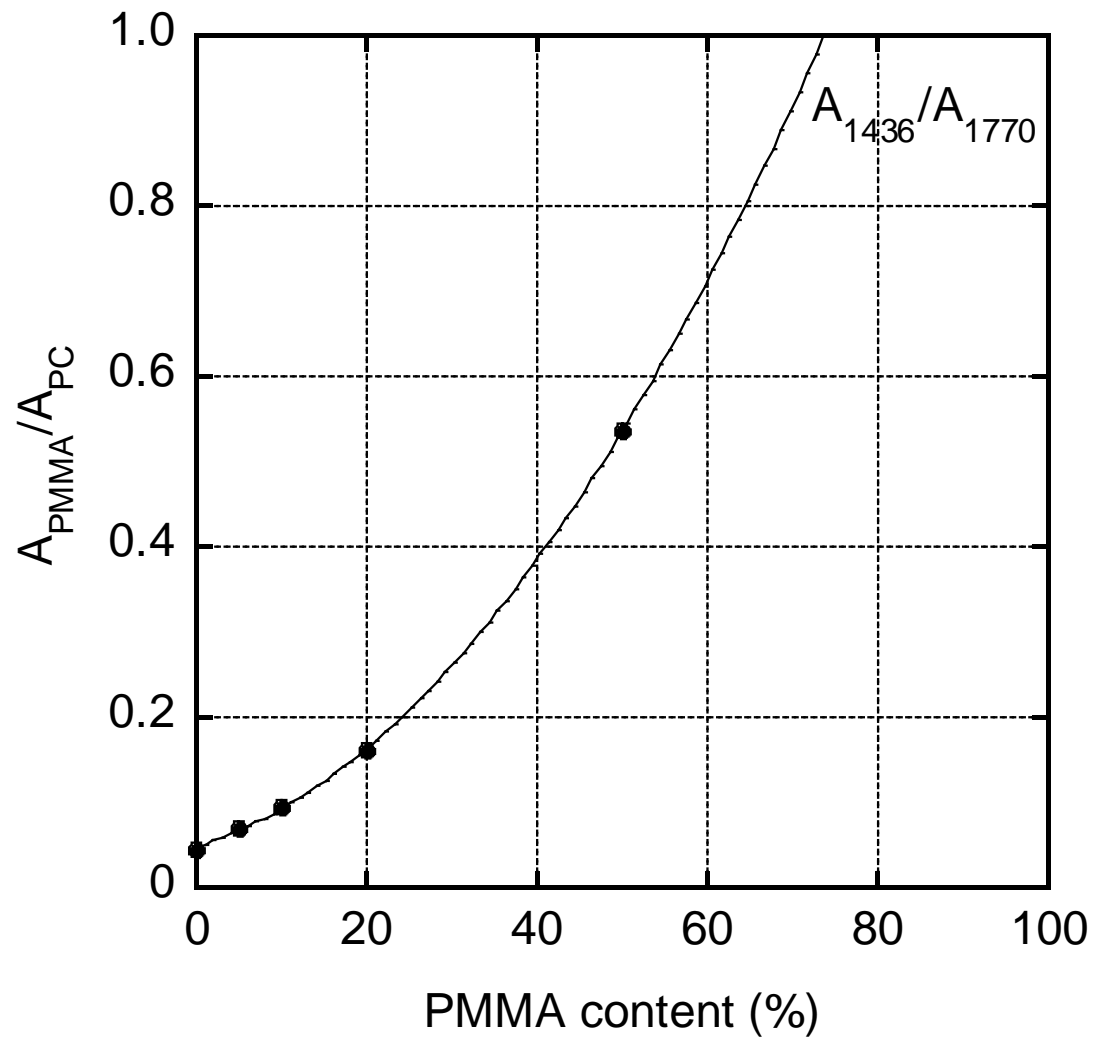


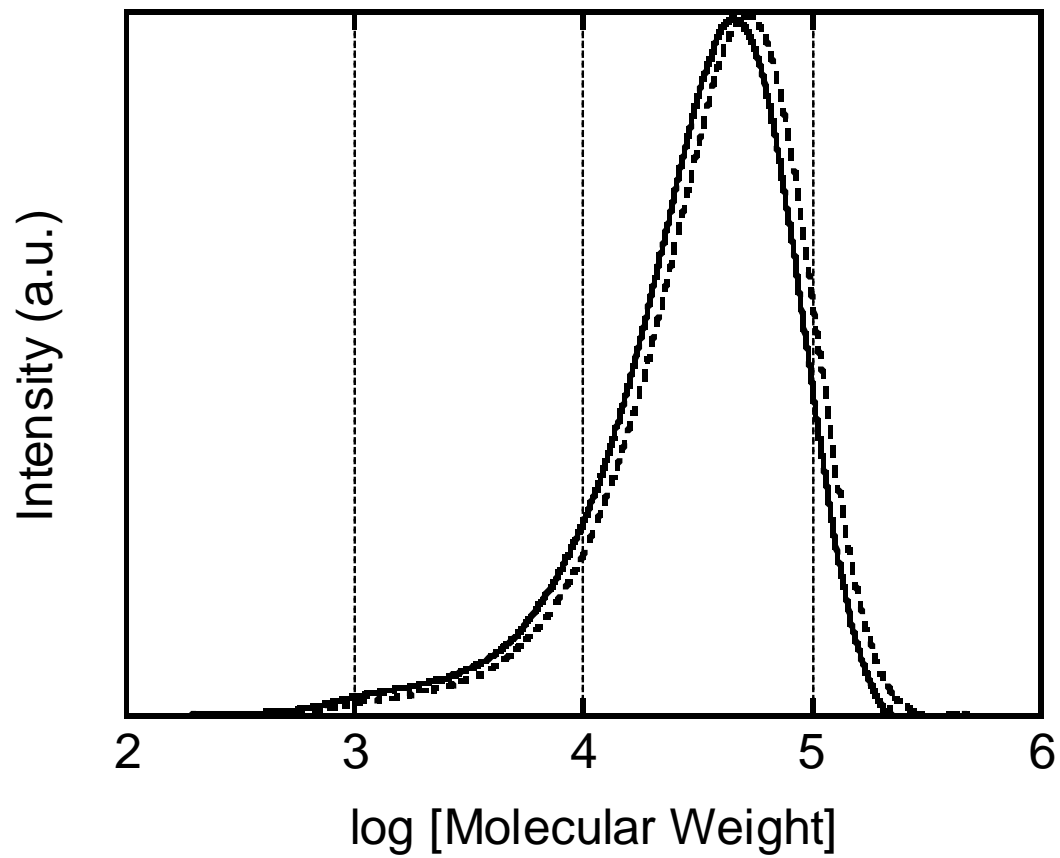




Sako et al., Figure 3







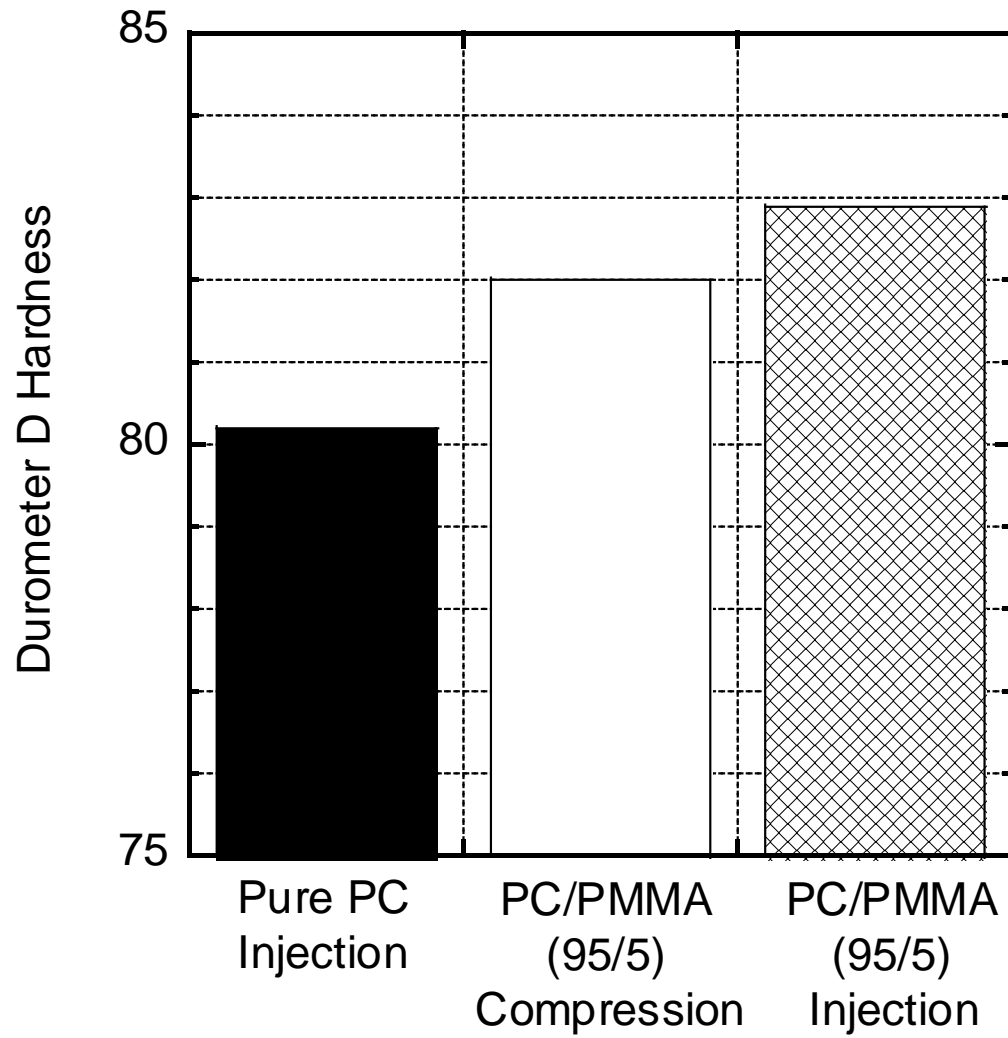


Table 1 Peak ratios and PMMA contents evaluated by ATR

Crystal	Point	$A_{1436}/A_{1770}$	PMMA content (%)
KRS-5	1	0.068	5.6
	2	0.072	6.5
Ge	1	0.099	12.0
	2	0.099	12.0